CONTRIBUTION OF MECHANICAL CONDITIONS TO MICROVASCULAR FORMATION IN EARLY PHASE OF CORTICAL DEFECT HEALING IN A CANINE MODEL

I Toda (1,2), N Inoue (1), Y Tamada (2), F Suwa (2), J Lim (1), V Wu (1), EYS Chao (1)

(1) Orthopaedic Biomechanics Laboratory
Johns Hopkins University
Baltimore, MD

(2) Department of Anatomy
Osaka Dental University
Osaka
Japan

INTRODUCTION

Cortical bone defect repair follows intramembranous ossification as a result of its stable mechanical condition [1]. Intramembranous ossification is termed "angiogenic ossification" by Krompecher [2], and a contribution of the initial vascular structure to the subsequent trabecular formation has been postulated [3]. Recent studies indicated the existence of vascular growth factors in the cortical bone and load induced fluid flow within the cortex. We hypothesize that the stress conditions in the cortex adjacent to the cortical defect affect the neovascular formation in the cortical defect and subsequent trabecular formation. This study analyzed the microvascular structure 1 week after creation of the defect and the subsequent trabecular formation. The origin and orientation of the microvascular structures were compared with the strain energy density in a Finite Element model (FEM) with the same cortical bone defect.

MATERIALS AND METHODS

Eight skeletally matured adult male canines were used for this study. Unilateral longitudinal rectangular cortical bone defects were created in the antero-medial surface of the mid-diaphysis of the tibia. Defect length was equal to the tibial outer diameter (1 OD) and the defect width was 0.25 OD. The corners of the defect had a 0.8 mm radius of curvature. The defect was created by connecting several drill holes using a fine osteotome. The drilling depth was set according to the thickness of the cortex, as measured by preoperative radiograms, to avoid damaging vascular structure in the medullary cavity. The dogs were euthanized 1 week after surgery for microvascular analysis (n=2) and 4 weeks after surgery (n=6) for trabecular structure analysis. The protocol was approved by Institutional Animal Care and Use Committee. A vascular corrosion casting method was used for the microvascular analysis [3,4]. Immediately after euthanasia, a physiological saline solution with heparin (500 U/100 ml) was infused the through the femoral artery. Thereafter, acryl plastic (Mercox, Dainihon Ink Chemicals) was infused. After extracting the diaphysis of the tibia, the tibia was cut transeversally at the middle of the defect. The proximal half was bisected in the sagittal mid-plane. Transverse sections were cut from the distal half of the specimen. The soft tissue in the specimens was digested with 5% sodium hypochlorite solution in 40 ?C water bath. After careful washing and drying, the bone-microvascular corrosion casts were coated with gold for scanning electron microscopic (SEM) study. For the trabecular analysis, contact micrograms were taken in a self-contained x-ray cabinet. The images were digitized and analyzed by 2-dimensional Fast Fourier Transform (FFT) to evaluate microvascular and trabecular orientation [5].

A FEM was assembled from digitized points from sequential CT scans through a canine tibia. A defect with a 0.25 OD width, a 1 OD length and 0.8 mm radius of curvature was created within the mid-diaphysis of the model. The strain energy density (SED) distribution was calculated for multiple loading conditions.

RESULTS

Microvascular analysis revealed two distinct capillary formations. The first one was that capillaries originated from the medullary canal towards the bone defect (Fig. 1-A, area 1). The second one was capillary formation from the endosteal surface towards the defect (Fig. 2-B, area 2). In the trabecular structure analysis, the intradefect trabeculae were oriented perpendicular to the long axis of the tibia (Fig. 3-C, area 3). In the medullary canal, trabecular orientation was from the endosteal surface towards the defect (Fig. 3-C, area 4). The direction and orientation of the trabecular structure at 4 weeks greatly coincided with those of the vascular formation at 1 week.

In the FEM, it was found that large SED concentrations and SED gradients were produced at the defect corners during torsion and bending loads (Fig. 4). Craniocaudal bending produced SED concentrations at two diagonal corners of the defect. Mediolateral bending produced SED concentrations at the opposite two corners. In comparing with the FEM, it appeared that regions with large SED gradients in the bone right after defect creation coincided with regions where capillaries were initiated from the endosteal surface.

DISCUSSION

The repair mechanism of cortical bone defects differs from that of fracture or osteotomy due to its stable mechanical condition and lack

of micromotion. Therefore, magnitude of the stress in hematoma or granulation tissue formed within the bone defect would be minimal until the calcified tissue was formed within the defect. However, the rectangular bone defect creates high stress gradient in the cortex around the defect, which had significant effect on woven bone formation in the repairing process [6]. The present study indicated that the capillary structure, which formed as early as 1 week after the creation of the bone defect, provided structural foundation for the subsequent trabecular formation in the defect. Microvascular formation from the medullary cavity towards the cortical defect might be governed by the pressure gradient and the concentration gradient of vascular growth factors in the hematoma formed in the cortical defect. Capillary formation was also observed from the endosteal surface adjacent to the defect where high SED was calculated. Stress induced vascular growth factor production and fluid flow may have contributed to initiate microvascular formation. Incorporation of the fluid flow model in the FEM may refine the relationship between the microvascular formation and stress conditions within the cortex surrounding the cortical defect.

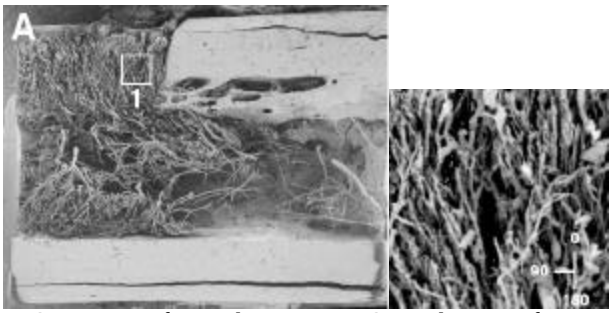

SEM image of sagittal section Original image 1 for FFT

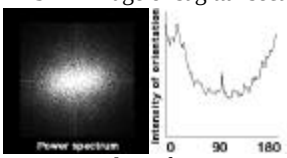

FFT analysis for area 1

Fig. 1 Scanning electron micrographs of the vascular casts of the sagittal section 1 week after surgery. Distribution of power spectrum and intensity of orientation as a function of angle (0-180 degrees) are shown for area 1.

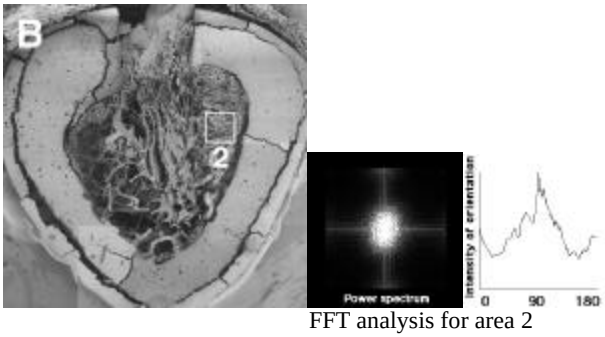

FFT analysis for area 2

Fig. 2 Scanning electron micrographs of the vascular casts of the transverse section 1 week after surgery. Distribution of power spectrum and intensity of orientation as a function of angle (0-180 degrees) are shown for area 2.

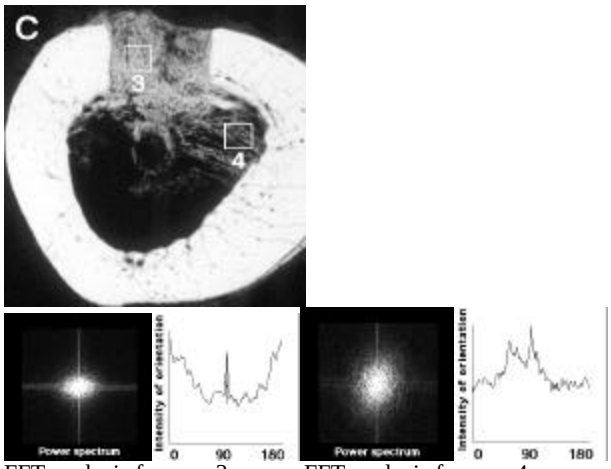

FFT analysis for area 3 FFT analysis for area 4

Fig. 3 Microradiogram of the transverse section 4 weeks after surgery. Distribution of power spectrum and intensity of orientation as a function of angle (0-180 degrees) are shown for selected areas 3 and 4.

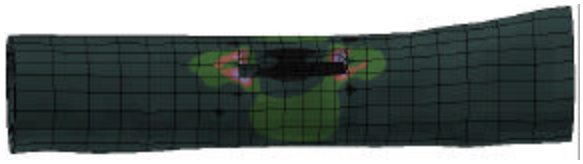

Fig. 4 Strain Energy Density distribution superimposed over the Finite Element model (0.25 width: 1.0 length) for a torsional load.

REFERENCES

1. Shapiro F (1988): JBJS 70A, 1067-81.
2. Krompecher S (1934): Verhand Anat Gesellshaft 42, 34-53.
3. Suwa F, et al. (1998): J Osaka Dent Univ 32, 27-34.
4. Ohta Y, et al. (1990): Okajima Folia Anat Jpn 66, 301-12
5. Inoue N, et al. (1995): Trans ORS 20, 523.
6. Elias JJ, et al. (2000): J Biomech 33, 1517-22.

ACKNOWLEDGEMENT

This work was supported in part by AO Research Project 2000-118 and US Army Medical Research and Material Command (USAMRMC, DAMD17-99-1-9239).